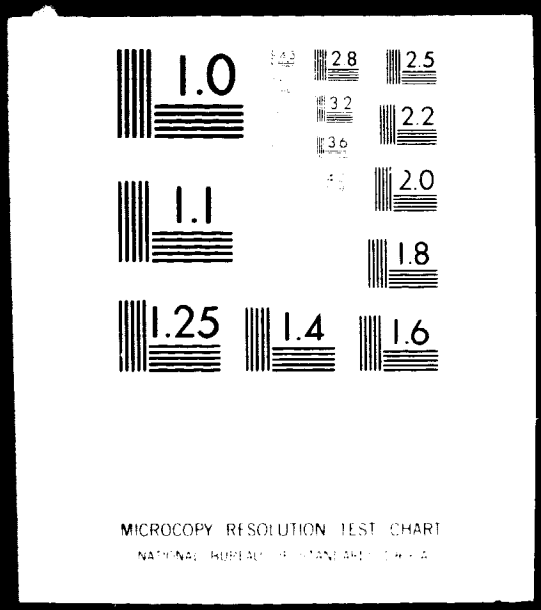

NASA TECHNICAL MEMORANDUM

NASA TM X-71614

NASA TM X-71614

PERFORMANCE OF A MODEL CASCADE THRUST REVERSER FOR SHORT-HAUL APPLICATIONS

by Donald A. Dietrich and Orlando A. Gutierrez
Lewis Research Center
Cleveland, Ohio 44135

TECHNICAL PAPER prepared for presentation at
Tenth Propulsion Conference cosponsored by
the American Institute of Aeronautics and Astronautics
and the Society of Automotive Engineers
San Diego, California, October 21-23, 1974

PERFORMANCE OF A MODEL CASCADE THRUST REVERSER FOR SHORT-HAUL APPLICATIONS

by Donald A. Dietrich* and Orlando A. Gutierrez*

National Aeronautics and Space Administration
Lewis Research Center
Cleveland, Ohio

ABSTRACT

Aerodynamic and acoustic characteristics are presented for a cowl-mounted, model cascade thrust reverser suitable for short-haul aircraft. Thrust reverser efficiency and the influence on fan performance were determined from isolated fan-driven models under static and forward velocity conditions. Cascade reverser noise characteristics were determined statically in an isolated pipe-flow test, while aerodynamic installation effects were determined with a wind-tunnel, fan-powered airplane model. Application of test results to short-haul aircraft calculations demonstrate that such a cascade thrust reverser may be able to meet both the performance and noise requirements for short-haul aircraft operation. However, aircraft installation effects can be quite significant.

E-8119

INTRODUCTION

The application of thrust reversing to short-haul aircraft operation differs from the case of conventional aircraft because of the shorter field length, higher thrust-to-weight ratio, and lower landing speeds of short-haul aircraft. The thrust reverser for these applications should be similar to those on present conventional aircraft in that it must generate sufficient reverse thrust to stop the airplane after touchdown, minimize the additional required weight, eliminate reingestion of hot exhaust flow, and avoid jet impingement on the ground. During the period of reversing, neither the engine operating point nor the internal flow quality should be adversely affected since this may result in reduced stall margin, reduced thrust, increased fan noise, and increased blade vibrational stress.

High thrust reversing efficiencies in conjunction with the higher installed thrust-to-weight ratio of short-haul aircraft can be used to advantage in reducing reverser-related noise; however, the general application of high efficiency reversers to an aircraft in terms of both performance and noise has not been considered previously. References 1 and 2 consider the aerodynamic performance of cascade thrust reversers applied to current high bypass ratio engines, but neither reference includes a discussion of the acoustic characteristics of an engine during the reversing operation. Reference 3 presents the acoustic characteristics of some model cascade thrust reversers and indicates that reverser noise levels can be very significant. This reference shows that reverser

*Aerospace Engineer, V/STOL and Noise Div., Member AIAA.

NASA TM X-71614
AIAA 74-1171

noise is a function of exhaust flow pressure ratio, cascade geometry, and reverser efficiency and that high-efficiency reversers produce less noise than low-efficiency reversers.

One way in which the reverser noise may be reduced is to reduce the engine power setting which reduces the engine noise, but this procedure requires a highly efficient thrust reverser so that the aircraft deceleration is sufficient for all stopping operations. In brief, a balance is required between thrust reverser efficiency, thrust reverser noise, and engine power setting in order to meet both the performance and noise goals.

The approach of this paper is first to consider a representative short haul aircraft in terms of ground deceleration performance and reverser requirements. From this analysis, the range of interest of reverser power settings are determined. Using an example reverser, data are shown to illustrate isolated fan/reverser thrust performance, the performance of four fan/reverser systems installed on a model airplane, isolated reverser noise characteristics, and the effect of the reverser on the operating characteristics and internal flow distortion of the model fan.

The material presented in this paper was obtained from four different test programs. All of the tests used the same small-scale cascade thrust reverser which had a geometric circumferential emission angle of 241.2° and a design turning angle of 135°. All of the tests except the measurement of noise characteristics used a model fan which was 14.0 centimeters in diameter and operated at a design pressure ratio of 1.25. The noise measurements were made by exhausting a supply of unheated air through the reverser. The installed reverser characteristics were determined using an airplane model which had four similar fan/reverser systems. Tests were conducted under static conditions and in a wind tunnel with free-stream velocities ranging up to 41 meters per second. The model fan rotational speed was varied from 60% to 100% of the fan design speed.

REVERSER OPERATING REQUIREMENTS

The first consideration of the reverser operating requirements is the deceleration performance of a short-haul aircraft, which is determined for assumed aerodynamic characteristics and runway conditions. The aircraft reversing effectiveness, ε, is defined as the difference per unit thrust-to-weight ratio in aircraft deceleration with the reversers operating and without the reversers operating, i.e.,

$$\varepsilon \equiv \frac{(a/g)_r - (a/g)_{nr}}{(T/W)_{to}} \tag{1}$$

Solving the force balance equation for the aircraft reversing effectiveness yields

$$\varepsilon = \frac{1}{(T/W)_{to}} \left\{ \left(\frac{a}{g}\right)_r - \frac{C_D \rho_o V_o^2}{2(W/S)} - \left(1 - \frac{C_L \rho_o V_o^2}{2(W/S)}\right) \mu \right\} \tag{2}$$

where the above terms are defined in the SYMBOLS list.

Figure 1 shows the required aircraft thrust reversing effectiveness, ε, as a function of the deceleration, $(a/g)_r$, for values of the parameters listed in Table I. As shown in figure 1, decreasing the forward velocity significantly increases the required reversing effectiveness for a fixed deceleration because of the reduced aerodynamic drag force. However, an opposing trend in introduced because a high thrust-to-weight ratio significantly reduces the required reversing effectiveness. Thus, short-haul aircraft with low landing speeds and high installed thrust present a design challenge for thrust reversing systems.

The thrust reverser efficiency, η_r, which is a measure of the internal flow performance and discharge angle of the cascade vanes, is defined as the ratio of the reverse thrust to the static ($V_o = 0$) forward thrust with the engine at the same power setting ($\eta_r = T_r/T_{f,a}$). Assuming no interactions between the thrust reverser and the other retarding forces, the reversing effectiveness, ε, can also be expressed as

$$\varepsilon = \frac{T_r}{T_{to}} \tag{3}$$

where the above terms are defined in the SYMBOLS list. Then from equation (3), the relationship between the engine thrust setting and the reverser efficiency becomes

$$\text{Engine thrust setting} = \frac{T_{f,a}}{T_{to}} = \frac{\varepsilon}{\eta_r} \tag{4}$$

Equation (4) is plotted in figure 2 for constant values of reversing effectiveness. The area between the curves shown on figure 2 encloses the range of reverser effectiveness derived from figure 1 for a deceleration, $(a/g)_r$, of 0.35. Figure 2 illustrates that reducing the engine thrust setting for the purpose of reducing noise or other reasons requires increased reverser efficiency to maintain the same aircraft deceleration.

A representative case, $\varepsilon = 0.3$, is shown on figure 2 as the median of the values shown in order to simplify the analysis. For the representative case, engine thrust settings for reversing of 1.0, 0.6, and 0.4, correspond to approximate reverser efficiencies of 0.30, 0.50, and 0.75, respectively, and are indicated by the solid symbols on figure 2. This range of reverser efficiency ($0.3 \leq \eta_r \leq 0.75$) specifies the range of interest in this paper. The values of the engine thrust setting (1.0, 0.6, and 0.4) will be used throughout this paper to illustrate the aerodynamic and acoustic characteristic of the model reverser/fan system.

APPARATUS

The data presented in this paper were obtained from four test programs: static internal aerodynamic tests on a single fan/reverser, wind-tunnel isolated fan/reverser thrust tests, installation effects on a four-fan airplane model in a wind tunnel, and single reverser acoustic tests. All of the tests used the same thrust reverser, and all except the acoustic tests used the same model fan.

Test Models

Thrust reverser. - The thrust reverser (fig. 3) consisted of eight replaceable, cascade sectors and two axial support rails located 180° apart. Each cascade sector subtended a circumferential flow angle of 40.5° and was replaceable by a solid sector which provided circumferential blockage of the flow. The data in this paper were limited to a single geometry where the total emission was through six cascade sectors. The reverser configuration had two solid (non-flow) sectors located at the bottom of the nacelle as shown in figure 3(a) and a total emission angle of 241.2°. The flow was turned into the cascade reverser by a blocker door which had a forward sloping surface of 45° and seals to prevent flow leakage axially (fig. 3(a)). The blocker door was axially translatable to provide a variation of the cascade length, b_c, and the open (exit) flow area of the thrust reverser.

The design of the cascade reverser blades was presented in reference 4 and reviewed briefly here. The impulse-type cascade blades (fig. 3(b)) had an airfoil shape with a maximum thickness of 15 percent of the blade

chord. The blade chord length and solidity were 1.27 centimeters and 1.3 respectively. The chord length is assumed to be about half that which would be expected on a full size engine installation. The design turning angle for the flow was 135° which required a camber of 110° and mean line slope at the trailing edge of 41° (fig. 3(b)). For an outlet flow angle of 135°, the reversing efficiency, η_r, would be expected to be about 0.7 (as indicated in ref. 4) and would be representative of the reverser required for low thrust setting ($T_{f,a}/T_{to} = 0.4$) operation described previously.

Model fan and inlets. - The fan had a rotor tip diameter of 14.0 centimeters, and at the design rotational speed of 35 800 rpm passed a mass flow of 2.49 kilograms per second at a pressure ratio of 1.25. The fan was driven by a tip turbine which, at the fan design speed, required a mass flow of 0.47 kilograms per second of unheated air at a pressure of 2590 kilonewtons per square meter in the turbine plenum. Further information on the basic fan was reported in references 5 and 6.

Two inlet arrangements were used during the aerodynamic performance test series: an extended bellmouth inlet plus recirculation barrier (fig. 4) for static tests and a flight-type inlet without a recirculation barrier (fig. 3(a)) for both static and wind tunnel tests. The bellmouth inlet was used only when the recirculation barrier was installed and located 4.3 fan tip diameters forward of the fan stator exit plane. The flight-type inlet (fig. 3(a)) had a symmetrical lip made up of quadrants of two 2:1 ellipses and an inlet contraction ratio (highlight-to-throat area ratio) of 1.29. With the short cowl inlet, the cowl from inlet highlight to stator exit had a length of 1.02 fan tip diameters (fig. 3).

Two cascade axial positions were investigated. The close-spacing configuration as shown in figure 3(a) gave the shortest length possible between the stator trailing edge and cascade leading edge for this model. The second configuration of the model which is not shown was accomplished by the addition of a 6.35-centimeter spacer between the cascade leading edge and the fan stator exit plane. The addition of the spacer changed the normalized spacing distance (b_s/d) from 0.10 to 0.52, where b_s is the distance between the stator trailing edge and reverser leading edge, and d is the fan duct diameter (15.2 centimeters).

Airplane model. - A three-view drawing of the airplane model with dimensional characteristics is presented in figure 5. The model had a high wing and no tail. The airfoil section of the wing was NACA 4415, and a double slotted flap with the last flap deflected 60° was used throughout the tests. The wing had a 0.3505-meter mean aerodynamic chord, a 25° quarter-chord sweep angle, a 2.54-meter span, a 0.8903 square meter planform area, and a 7.25 aspect ratio. Four under-the-wing fan/reverser assemblies were installed on the airplane model as shown in figure 5. The centerline of each fan was located two fan tip diameters

above a stationary flow splitter plate to simulate the relative location of the airplane with respect to the ground during a landing ground roll. The four fan/reverser models were the same as previously described.

Test Facilities and Instrumentation

Static test stand. - The indoor static test stand, shown in figure 4, was constructed to support the fan, reverser, inlet, and the recirculation shield between the reverser and inlet. The model centerline was located 1.2 meters from the floor and 2.8 meters from the side walls of the test area. A 1.2-by-2.4 meter recirculation barrier was used to prevent recirculation of the reversed flow and was located 3.8 fan duct diameters forward of the stator exit plane.

The stator exit station (fig. 3) was the primary measuring station and contained the most extensive instrumentation. At this location there were hub and tip static pressure taps and total pressure rakes. There were seven hub static pressure measurements and twenty tip static pressure measurements, with each static tap located circumferentially midway between stator trailing edges. These taps and the total pressure rakes were 0.28 centimeter downstream from the stator trailing edges. The seven total pressure rakes were also placed circumferentially midway between stator trailing edges. Each rake had five total pressure tubes located at centers of equal areas. Measurements of the static pressure on the surface of the cylindrical passage immediately downstream of the bellmouth inlet were used to determine the fan mass flow based on a total pressure recovery of unity in the bellmouth flow. Tests were performed over a range of fan rotational speed from 60 to 100% of the design rotational speed of the fan.

Acoustic test stand. - The noise data were taken on an outdoor acoustic test stand (ref. 3) designed to minimize internal noise. The reverser was mounted on the exit of the test stand as shown in figure 6. The model fan was not used in these tests. Compressed air was supplied to the reverser at near ambient temperature by a 20-centimeter diameter pipe. This pipe was equipped with a flow-measuring orifice, a remotely operated flow control valve, a noise muffler to minimize internal noise, and a straight run of piping ending at the thrust reverser, which was 1.6 meters above ground level. The noise data were measured by nine condenser microphones with individual wind screens located on a semi-circle of 4.6-meter radius centered on the middle of the reverser exit plane. These microphones were spaced at 20° increments from 20° to 180° from the pipe inlet centerline, at the same height above the smooth asphalt surface as the pipe centerline. Tests were conducted over a range of nozzle total pressure ratio from 1.15 to 2.5.

Low speed wind tunnel. - The features of the Lewis 9-by-15-feet low speed wind tunnel are detailed in reference 7. The installation of the model fan and thrust reverser in the wind tunnel for the isolated fan thrust performance tests was described in reference 4 and is shown in figure 7. A single component load cell was located in the model centerbody (see fig. 3) to measure the total axial force during wind tunnel tests. The high pressure air supply line was designed to minimize any extraneous force it could apply to the model. The isolated fan/reverser tests were performed at fan rotational speeds of 90 and 100% of the design fan rotational speed and over a range of free-stream velocities from zero to 30 meters per second.

The instrumentation on the four fan/reverser assemblies of the airplane model was the same as that for the isolated fan/reverser tests. The airplane model itself contained a fuselage-mounted, three-component balance to measure lift, drag, and pitching moment. Tests were performed over a range of fan rotational speed from 60 to 100% of the design fan rotational speed and over a range of free-stream velocities from zero to 41 meters per second.

RESULTS AND DISCUSSION

The results of the four test programs previously described are discussed separately in this section. The internal aerodynamic data are presented first and involve matching the reverser to the fan. The thrust performance of the isolated and installed fan/reverser systems are considered next together with calculations of aircraft performance based on these data. The presentation of reverser acoustic data concludes the discussion.

Effects of Cascade Variables on Fan Performance

This section is devoted to the selection of the reverser geometric variables and fan operating conditions that will be used throughout this investigation. First, the reverser cascade length (effective exit flow area) in conjunction with the reverser axial position is selected to match the reverser system to the forward-thrust operating line of the fan. The magnitude and character of the internal flow distortion which may also affect the selection of a reverser is also presented. Finally, the determination of the fan thrust setting and reverser-flow total pressure ratio is made. The fan thrust setting will be used in a later section on the isolated and installed fan/reverser thrust performance. Reverser flow total pressure ratio is necessary to relate the acoustic measurements to the calculated airplane performance.

Effect of cascade length and axial position. - First, selection is made of the remaining reverser geometric variables, which in this case

are the reverser axial position relative to the fan, and the cascade length (or reverser exit area). The reverser geometry should be selected such that it does not force the fan too far off the normal (forward thrust) operating line which may be specified by the value of the stator exit static pressure ratio (i.e., fan back pressure).

Shown in figure 8 is the arithmetic average of the stator exit static pressure data ratioed to the ambient pressure as a function of percent design speed, N/N_d, for each configuration. The data presented on figure 8 were used to select the cascade length which best matched representative forward thrust data (solid symbols) which were obtained from test results for the same model fan with the same flight-type inlet and a representative forward-thrust nozzle. There is a general trend for the stator exit static pressure to decrease with increasing rotational speed and with increasing cascade length, (b_c/d). For a given value of the cascade length parameter, b_c/d, increasing the normalized rotor spacing distance b_s/d from 0.10 to 0.52, significantly decreased the stator exit static pressure as can be seen by comparing parts a and b of the figure. Tests performed with the short cowl configuration (flagged symbols, fig. 8(a)) indicate that the stator exit static pressure was lower than the values obtained with the bellmouth inlet and recirculation barrier.

Since the short spacing configuration ($b_s/d = 0.10$) represented the most severe coupling between fan and reverser, figure 8(a) was used to select the value of normalized cascade length (b_c/d). A value of b_c/d of 0.58 was chosen for the balance of the tests as the best match of forward and reverse thrust data over the entire range of percent design rotational speed. Much of the data to be presented in this paper is restricted to the spacing distance, b_s/d, of 0.10 since it was the more severe case, but data for $b_s/d = 0.52$ are presented when significant differences in the two configurations are found.

Flow distortion. - The installation of a thrust reverser on a fan can produce fan duct flow distortion. Consequently, fan duct flow distortion may increase fan noise or blade vibrational stress. The data presented in this section illustrate the effect of the reverser on internal flow quality for the particular fan/reverser system tested. It is included to alert the reader to additional considerations involved in achieving reverser operational and noise goals. Furthermore, the level of the fan duct distortion, which could be different for a real engine, may well be an additional factor in specifying the reverser design or geometric variables.

The characteristics of the flow distortion at the outlet of the model fan are shown in figures 9 and 10. Figure 9 shows the stator exit static and total pressure ratios as a function of circumferential position. The figure presents data for two rotational speeds as obtained from the

configuration which had the more severe spacing ($b_s/d = 0.10$) and the bellmouth inlet. Both the extent of the blocked emission (non-flow sector) and the direction of fan rotation are noted. The stator exit static pressure ratios (fig. 9(a)) show that there is a large stator exit static pressure rise above the average value in the vicinity of the blocked area when $N/N_d = 1.0$, whereas for $N/N_d = 0.60$, the stator exit static pressure rise in relation to the average value is reduced. The static pressure has a much larger variation circumferentially than radially for both rotational speeds.

The circumferential variation of the stator exit total pressure (fig. 9(b)) is similar to that of the stator exit static pressure. However, in the case of the total pressure there is a significant variation radially. The data from the outer passage total pressure probe shows the most dramatic effect with a locally high value in the center of the blocked emission and drop just as the blade leaves the blocked area. Again for the case when $N/N_d = 0.6$, the variations in the stator exit total pressure are significantly reduced.

Figure 10 presents two total pressure profile distortion parameters (D_t and $D_{t,max}$) for the internal fan duct flow as a function of percent design speed, N/N_d. The parameter D_t is the standard deviation of the stator exit total pressures ratioed to the mass averaged total pressure, while $D_{t,max}$ is the difference between the maximum and minimum stator exit total pressures ratioed to the same average total pressure. Data from all the configurations with a normalized cascade length of $b_c/d = 0.58$ are shown. From comparison of the results of this figure, it is evident that increasing the normalized spacing distance from 0.10 to 0.52 significantly reduces the fan duct flow distortion parameters over the range of rotational speeds. A further characteristic of the aft-location ($b_s/d = 0.52$) configuration is that $D_{t,max}$ increases sharply with increasing rotational speed at the higher values of rotational speed. The short cowl configuration has the effect of a slight increase in both total pressure distortion parameters above those of the corresponding bellmouth configuration over the range of rotational speeds. Figure 10 also illustrates that the effect of operation at a reduced rotational speed is to significantly reduce the fan internal flow distortion. For the case of the close-spacing ($b_s/d = 0.10$) configuration, a reduction from 100 to 60% of the design rotational speed reduces $D_{t,max}$ from 0.21 to 0.08.

Model fan operating parameters. - With the reverser geometry specified, the percent design speed values required for the model fan to produce the thrust setting values selected previously for the reverser operation in the discussion of figure 2 can now be determined. The total-to-ambient pressure ratio, P_2/P_a, of the reversed flow is also required in order to analyze the noise data.

Figure 11 shows the ideal fan thrust setting (T/T_d) as a function of the percent design speed (N/N_d) for the reverser using the bellmouth inlet and the flight-type inlet. The thrust values are those calculated from the measured fan mass flow and the total pressure expanding ideally to ambient conditions. These thrust values are representative of the exhaust momentum flux available for thrust reversing. The data for the bellmouth inlet and the flight-type inlet are in good agreement with the forward thrust configuration as shown. For the purposes of this paper, the engine thrust setting ($T_{f,a}/T_{to}$) used in figure 2 and the ideal fan thrust setting (T/T_d) in figure 11 are essentially the same and are used as a measure of engine power setting. As stated previously in relation to figure 2, the comparison to be made in this paper is the effect of operating the fan/reverser system at engine thrust settings of 0.4, 0.6, and 1.0. These values are attained at about 60, 75, and 100 percent design speed respectively for the bellmouth inlet configuration.

Shown in figure 12 is the mass averaged total pressure ratio at the stator exit plane as a function of percent design speed. Data are shown for both the bellmouth inlet and flight-type inlet configurations, and again both are in good agreement with the forward thrust data. The total pressure ratio values corresponding to percent design speed values of 60, 75, and 100 were found to be about 1.08, 1.14, and 1.25, respectively.

A summary of the reverser geometry variables and the fan operating parameters are summarized in Table II.

Isolated Thrust Reverser Efficiency

This section is devoted to the discussion of the thrust reverser efficiency for a single isolated fan/reverser system tested in the low speed wind tunnel (fig. 7). The cascade thrust reverser has the same geometric parameters ($b_s/d = 0.10$ and $b_c/d = 0.58$) as those chosen in the previous section. Figure 13 presents the results of the i olated fan/reverser test in the form of thrust reverser efficiency, $_r$, as a function of the ratio of free-stream velocity, V_o, to the average fan outlet flow velocity, V_j. Specifically, the denominator of the velocity ratio should be the cascade discharge velocity. However, there was no reverser exit flow instrumentation available for this test, and the average fan outlet flow velocity was assumed to be representative of the reverser outlet velocity (i.e., perfect impulse flow across cascade). Values of V_j, as calculated from the measured total and static pressures at the stator exit plane within the fan, were determined by use of a correlation of the internal aerodynamic test results. The use of the V_o/V_j velocity ratio non-dimensionalizes the data as in reference 8 and permits a more comprehensive analysis of the results to be made than the discussion of reference 4.

The thrust reverser efficiency, η_r, in figure 13 was determined as the ratio of the measured fan/reverser system thrust to the measured static ($V_o = 0$) forward thrust of the forward thrust configuration (no reverser) at the same fan rotational speed. As indicated previously, the fan thrust measurement was made using a single component load cell aligned with the fan axis. A correlation between the calculated V_j values and the measured fan rotational speed was used to determine the average fan outlet flow velocity used in figure 13.

The interaction of the reverser flow and the free-stream flow is a very complex process that involves several distinct regimes. The solid symbol on figure 13 represents the value for the static ($V_o = 0$) reverser efficiency using the bellmouth inlet and recirculation barrier of figure 4 (data from ref. 6). At static conditions, a significant reduction of the reverser efficiency from 0.69 to 0.58 occurs when the barrier and bellmouth inlet are replaced by the flight-type inlet (fig. 3). This reduction in reverser efficiency is attributed to the recirculation of some of the exhaust flow (ref. 4).

The idealized variation of reverser efficiency for increasing values of V_o/V_j is shown by the dashed line which is the combination of the static (bellmouth inlet configuration) reverser efficiency and the ram drag ($\dot{m} V_o$). This idealized variation does not include the effects due to base drag and inlet losses. Initially as the V_o/V_j velocity ratio is increased, the reverser efficiency actually remains constant rather than increasing. In this region, the reverser flow is dominant over the free-stream flow and some of the reverser flow continues to be recirculated. The difference between the idealized variation and the data implies that the percentage of the exhaust flow being recirculated has increased with increased V_o/V_j in this region.

At a V_o/V_j ratio of approximately 0.17 (point A on fig. 13), the free-stream flow deflects the reversed exhaust flow sufficiently so that recirculation is eliminated. Once the recirculation of the exhaust flow is eliminated, the reverser efficiency becomes approximately 0.7 and increases with increasing free-stream velocity due to the increase in ram drag and base drag with forward speed. A similar result for a cascade thrust reverser was discussed in reference 8.

The effect of low rotational speed (or low thrust setting) operation on the thrust reverser efficiency during reversing is also illustrated by figure 13. During the reverser operation on an aircraft, the V_o/V_j ratio decreases from a relatively high value to a low value due to the deceleration of the aircraft. By operating the fan at a reduced rotational speed, the value of V_j is correspondingly decreased. Therefore, for a fixed landing speed, say 41 meters per second, the values of V_o/V_j are 0.27 and 0.37 for 100 and 60 percent design rotational speeds respectively. These two values are denoted on figure 13 by the symbols

B and C. Hence, from figure 13, reduced rotational speed operation has an initial reverser efficiency (when V_o = 41 meters per second) that is higher than the initial value for the high rotational speed operation. However, there are little data from the test in the recirculation-free region

The lower limit of the reverser operating range, as shown on figure 13, may be determined to be the value of V_o/V_j at which recirculation occurs with a significant reduction of reverser efficiency. The velocity at which recirculation occurs approaching from high values of V_o is defined as the recirculation velocity, V_{rc}. For the V_j values corresponding to percent design rotational speed of 100, 75, and 60, the values of the recirculation velocity (V_{rc}) are determined to be 27, 22, and 20 meters per second respectively. Therefore, reducing the fan thrust setting (percent design speed) also reduces the lower limit of the free-stream velocity at which recirculation occurs.

As shown on figure 13, the experimental data for reverser efficiency for the selected configuration fall within or above the range of desired values developed earlier (fig. 2). The minimum value of η_r achieved in the tests is 0 55 which exceeds the minimum required value of 0.3 by a comfortable margin. Values of η_r in excess of 0.7 are achieved for $V_o/V_j \geq 0.17$ This is consistent with the requirements for high reverser efficiency specified in the section on reverser operating requirements

Installed Thrust Reverser Efficiency

This section presents the results of experiments conducted with the airplane model with four fan/reverser systems installed. All of the fan/reverser systems had the same geometric parameters as previously selected (b_s/d = 0.10 and b_c/d = 0.58). The installed thrust reverser efficiencies are examined and compared to the results obtained with the isolated fan/reverser (fig. 13). The comparison between the installed and isolated thrust reverser efficiency determines the aircraft installation effect and can provide an early indication of the actual aircraft performance.

Figure 14 presents the airplane-model-installed thrust reverser efficiency as a function of the ratio of the free-stream velocity to the fan outlet velocity. Data are presented for each of the four fan/reverser systems on the airplane model. The thrust reverser efficiency, η_r, and the V_o/V_j velocity ratio were determined in the same manner as previously described in connection with figure 13. The relationship representing both the idealized thrust reverser efficiency and the results of the isolated reverser tests (fig. 13) are also shown.

The average static reverser efficiency ($V_o = 0$) for all four fans of the airplane model was reduced to $\eta_r = 0.42$ compared to $\eta_r = 0.58$ for the isolated configuration. This further reduction below that of the isolated configuration is due to an increased amount of recirculated exhaust flow. The increase in recirculated flow is caused by the close proximity of adjacent fans to one another and of the inboard fans to the fuselage (fig. 15(a)). Some loss in efficiency may also be due to the addition of the simulated ground plane to the model (splitter plate, fig. 5). The data for the airplane model have the same trends, however, as the data for the isolated reverser as shown. The reverser efficiency for both inboard and outboard fans remains at a uniform level for values of V_o/V_j below 0.22. For the values of $V_o/V_j < 0.20$, the reverser efficiencies of the inboard fans are below those of the outboard fans as shown by the curves representing the average inboard and average outboard efficiencies on figure 14. The lower efficiencies of the inboard fans in this region are due to the fuselage deflection of the exhaust flow (fig. 15(a)).

Figure 14 shows that at a value of approximately 0.22 (point A', fig. 14) the inboard and outboard fans display individual characteristics. At point A', the inboard fans show an abrupt increase in reverser efficiency similar to the isolated configuration while the values of η_r for the outboard fans remain unchanged. The value of V_o/V_j of 0.22 is then the recirculation velocity ratio (V_{rc}) for the inboard fans of the airplane model and is greater than the corresponding value for the isolated fan/reverser (point A). Similar to the consideration of the isolated fan/reverser, the airplane model recirculation velocities are 35, 29, and 25 meters per second for percent design rotational speeds of 100, 75, and 60 percent respectively.

For $V_o/V_j > 0.22$ for the inboard fans and $V_o/V_j > 0.28$ for the outboard fans, the reverser efficiencies increase with increasing V_o/V_j ratio. The increase in efficiency is due to the same causes as discussed in the case of the isolated fan/reverser. However, in this region of V_o/V_j values, the reverser efficiencies of the outboard fans remain below the values of the inboard fans due to the ingestion of the inboard fan exhaust by the outboard fan inlet (fig. 15(b)). The ingestion between adjacent fans is due to the relative location of the fan nacelles and wing sweep as shown in figure 15.

The data of figure 14 illustrate that the installation of reverser systems on an airplane can promote ingestion effects which result in sizeable losses in reverser efficiency. However, the values of the average reverser efficiency for the selected configuration still fall within or above the range of desired values ($0.3 \leq \eta_r \leq 0.75$) determined in the section on reverser operating requirements.

Calculated Aircraft Performance

This section uses the measured airplane-model data to calculate full-scale-aircraft deceleration values and ground roll distances. The calculations made in this section combine the airplane-model installation effects (preceeding section) with the interaction effects between the reverser flow and aircraft aerodynamics. The results of these calculations indicate the ability of an aircraft with the selected reverser to land on a short runway typical of short-haul operations.

Aircraft deceleration values. - Shown in figure 16 are predicted aircraft deceleration values, $(a/g)_r$, as a function of free-stream velocity, V_o. The predicted aircraft deceleration is determined using the equation:

$$\left(\frac{a}{g}\right)_r = \frac{C_D' q}{W/S} + \mu\left(1 - \frac{C_L' q}{W/S}\right) \tag{5}$$

where C_D' and C_L' are obtained from balance measurements made with the airplane model. The coefficients C_D' and C_L' are different from the aerodynamic force coefficients, C_D and C_L, which were used in the section on reverser operating requirements since C_D' and C_L' are based on the total forces including the effects of the thrust reversers. The $(a/g)_r$ values are determined by assuming that C_L' and C_D' measured on the airplane model apply directly to a full-scale aircraft having a wing loading, W/S, of 100.

Figure 16(a) and 16(b) present the data for assumed constant runway friction coefficients, μ, of 0.4 and 0.15 respectively. These runway friction coefficients represent measured values of moderate to very low values (ref. 9). Data are presented for percent design speeds of 60, 75, and 100%. For all values of friction coefficient and rotational speed, the data are shown to have a linearly decreasing deceleration with decreasing free-stream velocity for the higher values of the free-stream velocity. For the lower values of the free-stream velocity, the deceleration rates are shown to be constant.

For a friction coefficient of 0.4 (fig. 16(a)), the deceleration values for all rotational speeds and free-stream velocities are very high, with a minimum value of $(a/g)_r = 0.45$. Therefore, for moderate to high values of μ, the values of the aircraf deceleration exceed the previously selected range of interest ($0.3 \leq (a/g)_r \leq 0.4$). The results of figure 16(a) indicate that for $\mu \geq 0.4$, the aircraft can be decelerated with reduced rotational speed operation which also implies reduced noise. Furthermore, partial braking combined with low rotational speed operation of the reversers can be used to obtain $(a/g)_r$ values

between 0.3 and 0.4. The results of these calculations are much different, however, for a friction coefficient of 0.15 (fig. 16(b)). For $\mu = 0.15$, some of the deceleration values are less than 0.30, with a minimum value of $(a/g)_r = 0.20$ for a 60% fan design rotational speed. In this case, it is not clear that the aircraft can meet the previously determined requirements. Therefore, calculations of the ground roll distance for the case when $\mu = 0.15$ are required to determine the suitability to short-haul applications.

Ground roll distance. - The aircraft deceleration results for $\mu = 0.15$ of the previous section could not alone determine the effect of using the selected reverser system on a runway having a low friction factor. This may be done by knowing the ground roll distances over the range of rotational speeds.

Calculated ground roll distances for the lower runway friction factor ($\mu = 0.15$) are shown in figure 17. The results are plotted against the reverser termination velocity, V_t, which is defined as the lower limit of the free-stream velocity to which the reversers are used. The ground roll distance is determined by use of the equation:

$$X = \frac{1}{g}\int_{V_{td}}^{V_t} \frac{V\,dV}{(a/g)_r} + \frac{1}{g}\int_{V_t}^{0} \frac{V\,dV}{(a/g)_{nr}} \tag{6}$$

where $(a/g)_r$ and $(a/g)_{nr}$ are determined from model balance measurements with the reversers operating and without the reverser operating, respectively. The $(a/g)_r$ values are shown on figure 16(b). The deceleration values without the reversers operating, $(a/g)_{nr}$, were determined by performing a wind tunnel test with the cascade reverser removed from the model airplane and the model fans unpowered.

The results of equation (6) are shown in figure 17 for three fan percent design speeds and an assumed aircraft touchdown (reverser initiation) velocity of 41 meters per second. As may be seen from figure 17, the ground roll distance increases as the reverser termination velocity increases. As expected, the effect of percent design speed becomes less significant as the reverser termination velocity increases.

For the assumed representative deceleration rate of 0.35 is assumed, the ground roll required to stop the aircraft initially at 41 meters per second is 245 meters. This value of 245 meters is representative of the goal which would be derived from the discussion of the reverser

operating requirements (figs. 1 and 2) and is shown on figure 17 by the dashed line. As shown on the figure, this goal can be met by operating the fan reversers at the design rotational speed ($N = N_d$) down to a reverser termination velocity of about 8 meters per second. This procedure, however, would require operating the aircraft in the region of reverser exhaust recirculation and at a high noise level.

If either fan operation during recirculation or reverser noise level (due to high rotational speed and high total pressure ratio) cannot be accepted, the ground roll distance exceeds the distance goal. The solid symbols on each line of constant rotational speed represent the point at which recirculation occurs for the airplane model ($V_o/V_j = 0.22$, fig. 14). If the reverser termination velocity is selected (as in the case of conventional aircraft) to be the same value as the recirculation velocity, then it is clear from figure 17 that the required ground roll distance is greater than the desired value of 245 meters in all cases. For the selected reverser, it is interesting that, for the case when $V_{te} = V_{rc}$, the shortest ground roll distance is obtained by using the lowest value of the fan percent design speed ($N/N_d = 60\%$). This effect of the use of low percent design speed operation is opposite that which would be expected. In this case, the ground roll distance is 365 meters or about a 50% increase over the goal value of 245 meters. Since the example being considered ($\mu = 0.15$) is such an extreme or infrequent case, this result may well be acceptable to short-haul aircraft operation.

Reverser Acoustic Results

The material previously presented assumed that the combination of a high efficiency thrust reverser and low thrust setting operation of the engine would meet both the performance and noise goals for a short-haul aircraft. Previous sections have dealt with the aerodynamic performance of the reverser, and this section is devoted to the noise generated by the same thrust reverser. Even though the model fan is not included in the acoustic test results, the thrust reverser is identical to that of the previous sections and to one of the reverser configurations of reference 3. As indicated previously, the cascade thrust reverser had a total emission angle of 241.2° (fig. 3(a)) and normalized cascade length, b_c/d, of 0.58. The data reported here are restricted to the selected thrust reverser geometry over the operating range of interest. However, a detailed acoustic study of this reverser along with other configurations is presented in reference 3.

The acoustic data presented in this paper include sound power level spectra and overall sound power level values. The results are scaled to estimated full-scale engine sideline perceived noise in order to evaluate the application of the reverser to a short-haul airplane.

Sound power level. - A notable feature of the results for the selected thrust reverser is the presence of high frequency narrow band noise in the sound power level spectra in the 5 to 8 KHz region (ref. 3). The natural frequency of the reverser cascade was measured as 8.4 KHz. Hence, it is highly probable that the narrow band noise is caused primarily by a mechanical resonance of the cascade. A similar observation is made in reference 3. However, it is suspected that the origin of noise may be complicated by sources in addition to mechanical resonance and that further analysis is needed to verify the preliminary conclusion of mechanical resonance.

Since these mechanical vibratory tones would most likely not be present in an actual installed configuration, the narrow band acoustic spectra (sound pressure level values which were also recorded) were modified by smoothing the data in the region of concern. The modified narrow band spectra and the data of reference 3 for the sound power level spectra were then used to generate adjusted 1/3-octave sound power level spectra. Figure 18 presents the adjusted sound power level spectra for the selected reverser for total pressure ratios across the cascade reverser (P/p_a) of 1.39, 1.25, and 1.15. The data points that were modified by the smoothing techniques are shown on figure 18 as flagged symbols. The reverser total pressure ratio, P/p_a, is based on a measurement well upstream of the reverser but is essentially the same as the stator exit average total pressure ratio, P_2/p_a, of the model fan tests. As shown in Table II, the latter two pressure ratios (1.25 and 1.15) correspond approximately to 100 and 75 percent fan design speeds, respectively, for the fan/reverser configuration.

Figure 18 indicates that the sound power level decreases with decreasing total pressure ratio. This is a beneficial trend in the data since it indicates that noise levels of reversers can be reduced by reducing the pressure ratio of the engine (e.g., power setting). It can also be seen in figure 18 that the peak power is shifted toward higher frequencies as the total pressure ratio is increased.

Test data are not available for a reverser total pressure ratio of 1.08 which corresponds to the low rotational speed operation of the model fan/reverser (60% fan design speed). An estimation of the noise at the low total pressure ratio was made by considering the overall sound power level. Values of the normalized overall sound power level, OAPWL, are shown in figure 19. The variation of the OAPWL values are shown as functions of the normalized jet velocity, V_j/c_a, and reverser total pressure ratio, P/p_a, for a wide range of pressure ratios. The symbols on figure 19 represent the adjusted spectra with the narrow band noise removed (fig. 18). Also shown for reference on figure 19 are data for a convergent nozzle. The data for the modified spectra display a uniformly decreasing overall sound power level with decreasing reverser pressure ratio. This behavior of the data permits an estimate

(by extrapolation) to be made for the OAPWL for the 1.08 total pressure ratio which will be used in a subsequent section of this paper.

Full-scale perceived noise level. - The adjusted acoustic data of the selected reverser configuration were then used to predict full-scale aircraft sideline noise. Figure 20 presents the estimated reverser sideline perceived noise level in PNdB for a single full-scale engine as a function of the distance in meters behind the aircraft along a 152-meter sideline. The curves of figure 20 include the data for nozzle pressure ratios of 1.25 and 1.15 which correspond to 100 and 75 percent fan design speeds respectively for the fan/reverser configuration. The PNdB values were calculated using the method of reference 3 with the sound intensity levels obtained for the model tests scaled directly with area to a fan having a diameter of 1.96 meters compared to 0.18 meters for the model. To scale the frequencies it was assumed that the frequency varies inversely with the spacing distance between cascade blades, and that a full-scale cascade reverser would have blades twice the size (and spacing) of the model.

As shown in figure 20, the maximum values of the sideline noise are 106.0 and 101.3 PNdB for total pressure ratios of 1.25 and 1.15, respectively. Also shown is an estimated peak sideline noise value of between 97 and 98 PNdB for a 1.08 total pressure ratio. This latter value was estimated by assuming that the change in peak PNL with pressure ratio was equal to the change in overall sound power level (fig. 19). Also shown in figure 20 is the target value of 100 PNdB which represents the sideline noise goal for a short-haul aircraft.

The results of figure 20, which were calculated from the isolated model reverser data, indicate that lower noise levels can be achieved by reducing the reverser total pressure ratio, i.e., by reducing the thrust setting. However, the entire aircraft must meet the 100 PNdB sideline noise goal. If it is assumed that the fuselage completely shields the sideline noise from two of the four engines, then approximately 3 dB should be added to the values of figure 20 to be representative of the aircraft sideline noise. The full-scale aircraft noise goal is approached only for the low pressure ratio case (P/p_a = 1.08 or N/N_d = 60%). This result, when combined with the results of figure 16(a), implies that both the performance and noise goals can be met under normal conditions using the selected reverser and low thrust setting operation. For the extreme case of the low runway friction coefficient (figs. 16(b) and 17), the results indicate that either the noise goal or the nominal ground roll distance would be exceeded in stopping the aircraft.

The preceeding results assume that the acoustic characteristics are not changed by airplane installation effects, contrary to the case of the aerodynamic performance results. This may not be the case, and additional acoustic tests of the airplane model are required. However, if the sideline noise is adversely effected by installation effects, additional

acoustic suppression gains may also be possible by selecting the chord or spacing of the reverser cascade such that the frequencies of the maximum sound pressure level fall in a frequency range that contributes less to the PNdB value. In addition, further reductions in the reverser noise may be achieved by improving the internal aerodynamics of the flow in the fan/reverser system, reducing the cascade length (i.e., reducing the reverser exit areas as in reference 3), and using noise-shielding panels (ref. 3).

SUMMARY OF RESULTS AND CONCLUDING REMARKS

Four experimental investigations of the performance of a cowl-mounted, cascade thrust reverser suitable for short-haul aircraft were conducted. The tests were performed to determine the effect of the thrust reverser on model fan operating conditions, isolated fan/reverser thrust performance, installed reverser performance on a powered airplane model, and acoustic characteristics without a model fan. This paper considered only one cascade thrust reverser which included highly cambered, contoured blades and a partial circumferential emission pattern of 241°. The main results of these investigations may be summarized as follows:

1. The tests of the isolated fan/reverser indicate that recirculation of the reverser exhaust flow by the fan significantly reduces the thrust reverser efficiency.

2. High reverser efficiencies (greater than 0.7) can be achieved at low fan thrust settings (engine power settings).

3. Installing the thrust reversers on a model four-fan airplane produces further reductions in reverser efficiency. These installation losses were attributed to the recirculation of the exhaust flow and the ingestion of the inboard fan exhaust by the outboard fan. The reversers installed on the model airplane display the same trends of reverser efficiency with forward velocity as the isolated reverser. However, the inboard and outboard reversers exhibit individual behavior patterns.

4. Acceptable full-scale aircraft deceleration and ground roll performance can be attained with the cowl mounted cascade reverser when operated at low thrust settings under normal operating conditions.

5. Decreasing the thrust or power setting reduces the noise output of the reverser. It is estimated that for the subject reverser a full-scale aircraft operating at a 40% thrust setting can achieve a 152-meter perceived sideline noise goal of 100 PNdB.

6. For the case of a very low runway friction factor (μ = 0.15), either the nominal ground roll distance or the aircraft noise goal would be exceeded in stopping the aircraft.

This paper has demonstrated that cowl-mounted cascade thrust reversers have the potential of achieving desired aerodynamic and acoustic performance goals of a short-haul aircraft. These goals may be achieved by the use of a high-efficiency thrust reverser in combination with engine operation at a reduced thrust (power) setting. However, the possibility of further gains in reverser performance and reductions in reverser noise is suggested by the results of this paper. For example, the installed thrust reverser efficiency can be increased by properly locating the reversers on the aircraft or changing the reverser exhaust pattern to reduce ingestion from adjacent engines. Further analysis may also be done on the observed reverser narrow band noise and the internal fan duct flow so that these additional noise sources can be eliminated. In addition, other reverser geometries of references 3 and 4 which demonstrated high reversing efficiency and low noise independently should be considered in a fashion similar to approach of this paper. Further tests of this type are encouraged.

SYMBOLS

A_e	equivalent flow area of reversed flow, $\dot{m}/\rho_a V_j$, m^2
a/g	aircraft deceleration as a fraction of the acceleration due to gravity
b_c	cascade length (distance from the leading edge of the initial cascade blade to the blocker door), m
b_s	stator-reverser spacing distance (distance from stator exit to cascade inlet), m
C_D	aerodynamic drag coefficient, aerodynamic drag/qS
C_D'	airplane-model-measured drag coefficient, drag (including reverse thrust)/qS
C_L	aerodynamic lift coefficient, aerodynamic lift/qS
C_L'	airplane-model-measured lift coefficient, lift (including effect due to reverse thrust)/qS
c_a	speed of sound at ambient conditions, (static tests), m/sec
D_t	stator exit total pressure distortion parameter, (standard deviation of total pressure)/(average total pressure)
$D_{t,max}$	stator exit total pressure distortion parameter, (maximum total pressure - minimum total pressure)/(average total pressure)
d	fan duct diameter, 15.2 cm
d_t	fan tip diameter, 14.0 cm
f_c	1/3 octave band center frequency, Hz
g	acceleration due to gravity, 9.8 m/sec^2
$\dot{m}$	fan duct mass flow, kg/sec
N	model fan rotational speed
N_d	model fan design rotational speed, 35 800 rpm

N/N_d	fraction of design rotational speed, percent
OASPWL	overall sound power level, dB re 10^{-13} watts
P	total pressure, N/m^2
PNL	perceived noise level, PNdB
PWL	sound power level for each 1/3 octave band, dB re 10^{-13} watts
p_a	ambient pressure (static tests), N/m^2
p_s	static pressure, N/m^2
q	free-stream dynamic pressure, $\frac{1}{2}\rho_o V_o^2$
S	wing area, m^2
T	thrust, N
T_{to}	static ($V_o = 0$) thrust for engine at takeoff power setting
T/W	thrust to weight ratio
V_j	fully expanded ideal reversed jet velocity, m/sec
V_o	aircraft forward velocity during ground roll (free-stream velocity), m/sec
V_{rc}	reverser flow recirculation velocity (free-stream velocity at which the onset of recirculation occurs), m/sec
V_t	reverser termination velocity (free-stream velocity at which the reversing operation is terminated), m/sec
V_{td}	aircraft touchdown or landing velocity, m/sec
W	aircraft weight, N
W/S	aircraft wing loading
X	aircraft ground roll distance, m

ε	aircraft reversing effectiveness, $((a/g)_r - (a/g)_{nr})/(T/W)_{to}$
η_r	thrust reverser efficiency, $T_r/T_{f,a}$
μ	runway friction coefficient
ρ	air density, kg/m^3

Subscripts:

a	ambient conditions (static tests)
d	model fan design operating condition (with bellmouth inlet)
f	condition during forward thrust operation
nr	condition during ground roll without use of thrust reversers
o	condition in free-stream flow
r	condition during reverse thrust operation

REFERENCES

1. Thompson, J. D, "Thrust Reverser Effectiveness on High By Pass Ratio Fan Powerplant Installations," SAE Paper 660736, 1966.

2. Wood, S. K. and McCoy, J, "Design and Control of the 747 Exhaust Reverser Systems," SAE Paper 690409, 1969.

3. Gutierrez, O. A., Stone, J. R. and Friedman, R., "Results from Cascade Thrust Reverser Noise and Suppression Experiments," AIAA Paper 74-46, 1974.

4. Dietrich, D. A. and Luidens, R. W., "Experimental Performance of Cascade Thrust Reversers at Forward Velocity," TM X-2665, 1973, NASA.

5. "Performance of a 5.5-Inch Diameter Axial Fan with Various Inlets and Exits," Rept. 708-1, 1970, Tech. Development, Inc.

6. Lopiccolo, R. C., "Tests of Cascade Thrust Reversers on a 5.5-Inch Diameter Axial Fan," Rept. 789, 1971, Tech. Development, Inc.

7. Yuska, J. A., Diedrich, J. H. and Clough, N., "Lewis 9-by 15-Foot V/STOL Wind Tunnel," TM X-2305, 1971, NASA.

8. "C-5A(CX-HLS) Propulsion Design Verification Test Programs," 1965, General Electric Co.

9. Yager, T. J., Phillips, W. P. and Horne, W. B., "A Comparison of Aircraft and Ground Vehicle Stopping Performance on Dry, Wet, Flooded, Slush-Snow-and Ice-Covered Runways," TN D-6098, 1970, NASA.

Table I. Assumed Aircraft Characteristics During Thrust Reversing

Symbol	Value	Remarks
C_D	0.5	Typical values
C_L	0	
W/S	100	
μ	0.15	Wet/icy runway or partial braking
$(T/W)_{to}$	0.4,0.6	Range for short haul aircraft
V_o	0,41 meters per second	Static and touchdown (landing) conditions

E-811)

Table II. Reverser Geometry and Fan Operating Parameters

Reverser geometric parameters	Fan operating parameters		
——	Thrust setting, T/T_d	Percent-design speed, N/N_d	Total pressure ratio, P_2/P_a
Spacing ratio: $b_s/d = 0.10$	0.4	60	1.08
Cascade length: $b_c/d = 0.58$	0.6	75	1.14
	1.0	100	1.25

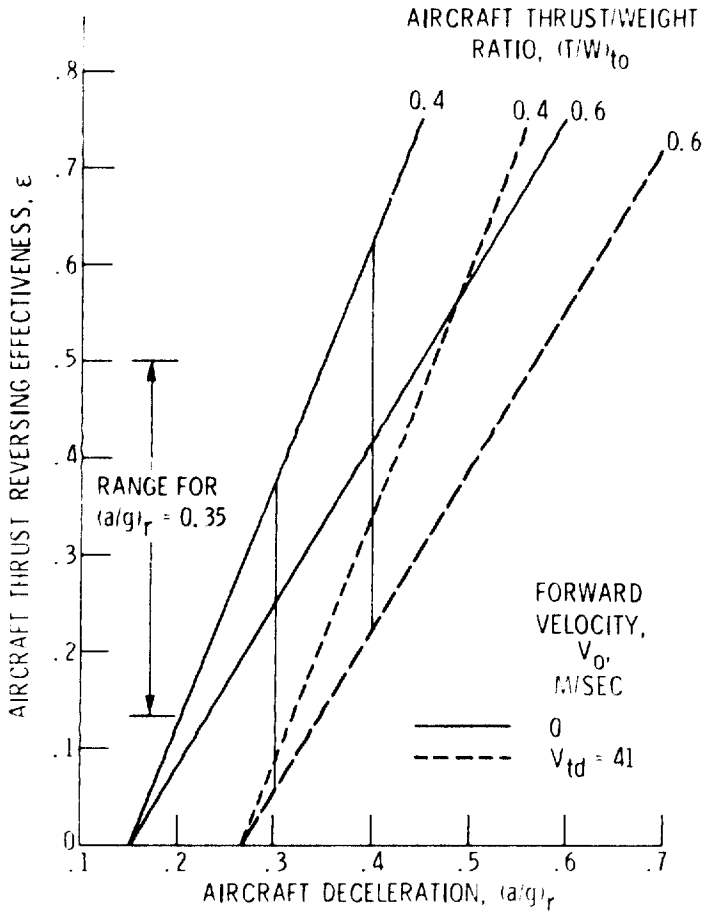

Figure 1. - Required aircraft thrust reversing effectiveness as a function of deceleration. C_D = 0.5, C_L = 0, W/S = 100, μ = 0.15.

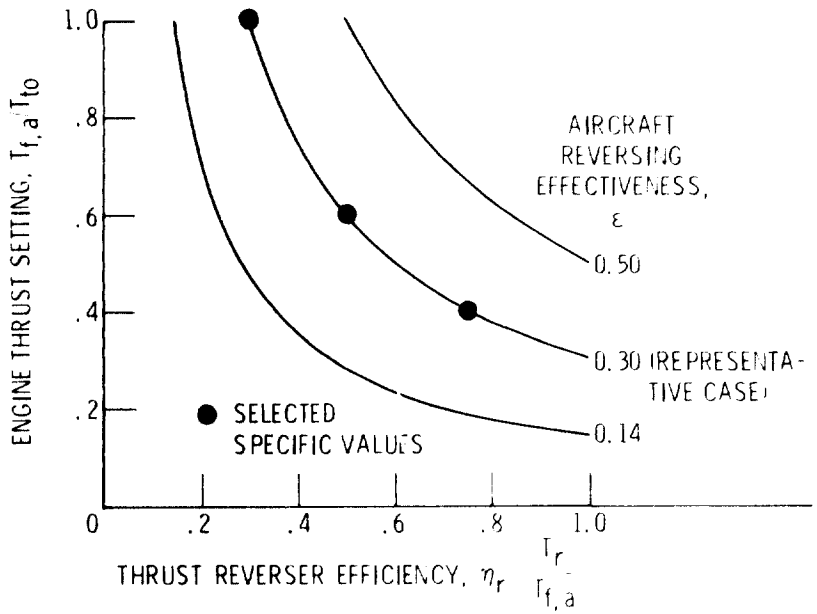

Figure 2. - Relationship between engine thrust setting and thrust reverser efficiency for constant values of aircraft reversing effectiveness for operating range of interest.

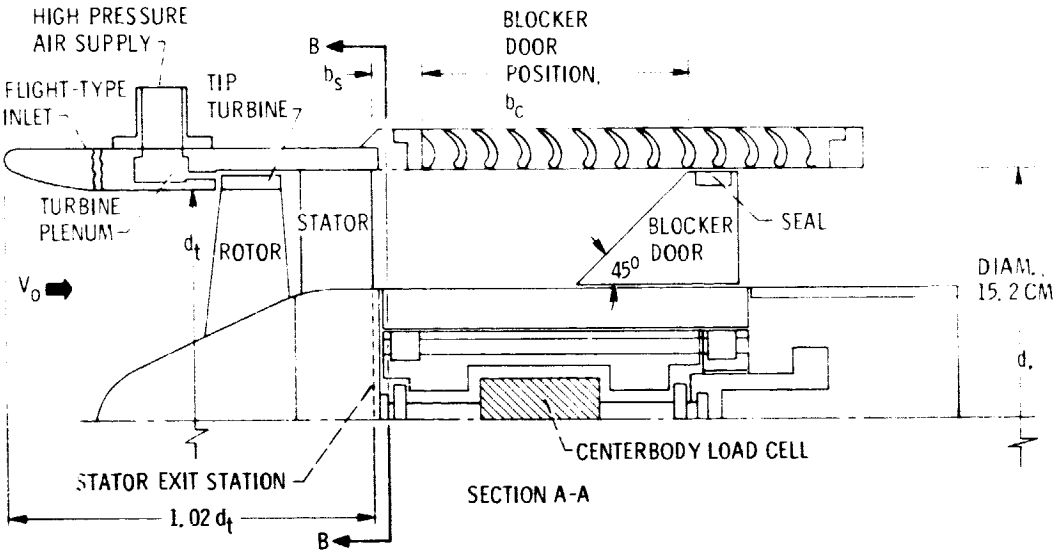

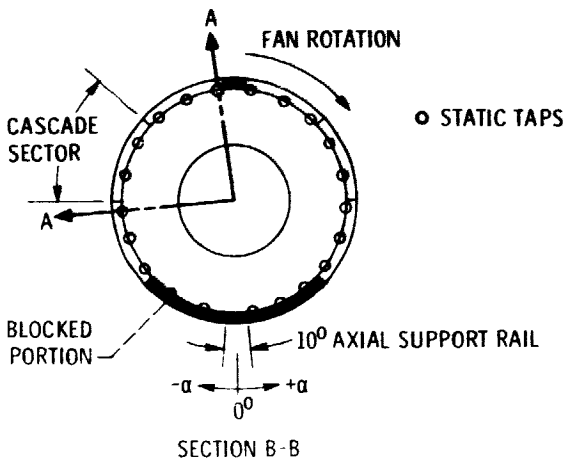

SECTION B-B

(a) FAN, INLET, AND THRUST REVERSER SECTION.

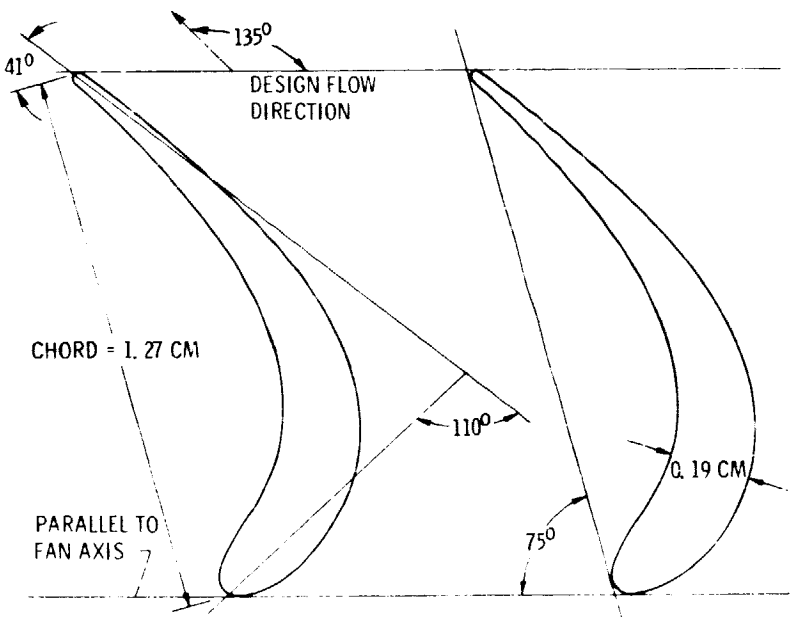

(b) THRUST REVERSER BLADE SECTION.

Figure 3. - Fan/Reverser model.

E-8119

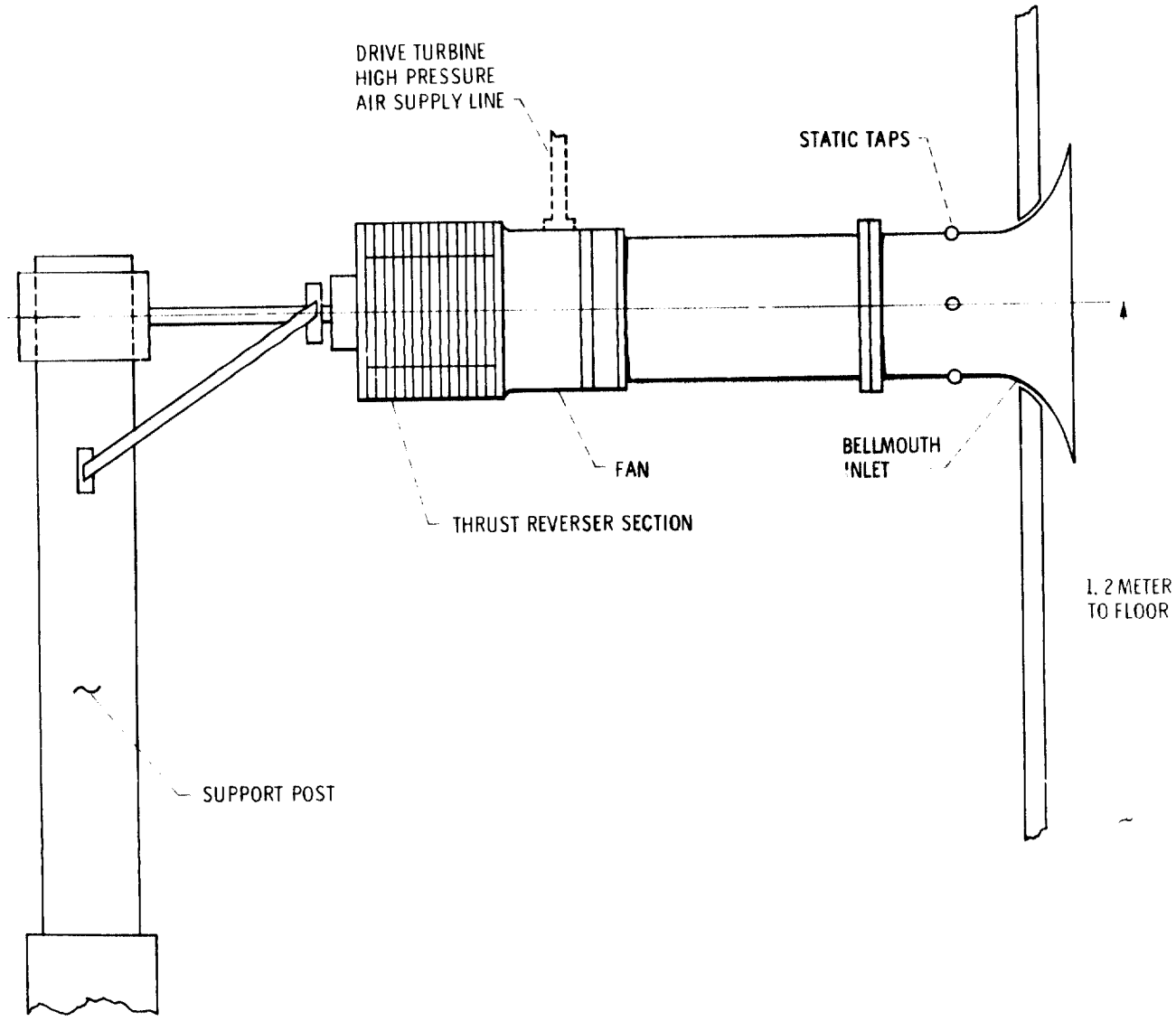

Figure 4. - Fan/reverser model including the bellmouth inlet and recirculation barrier on the static test stand.

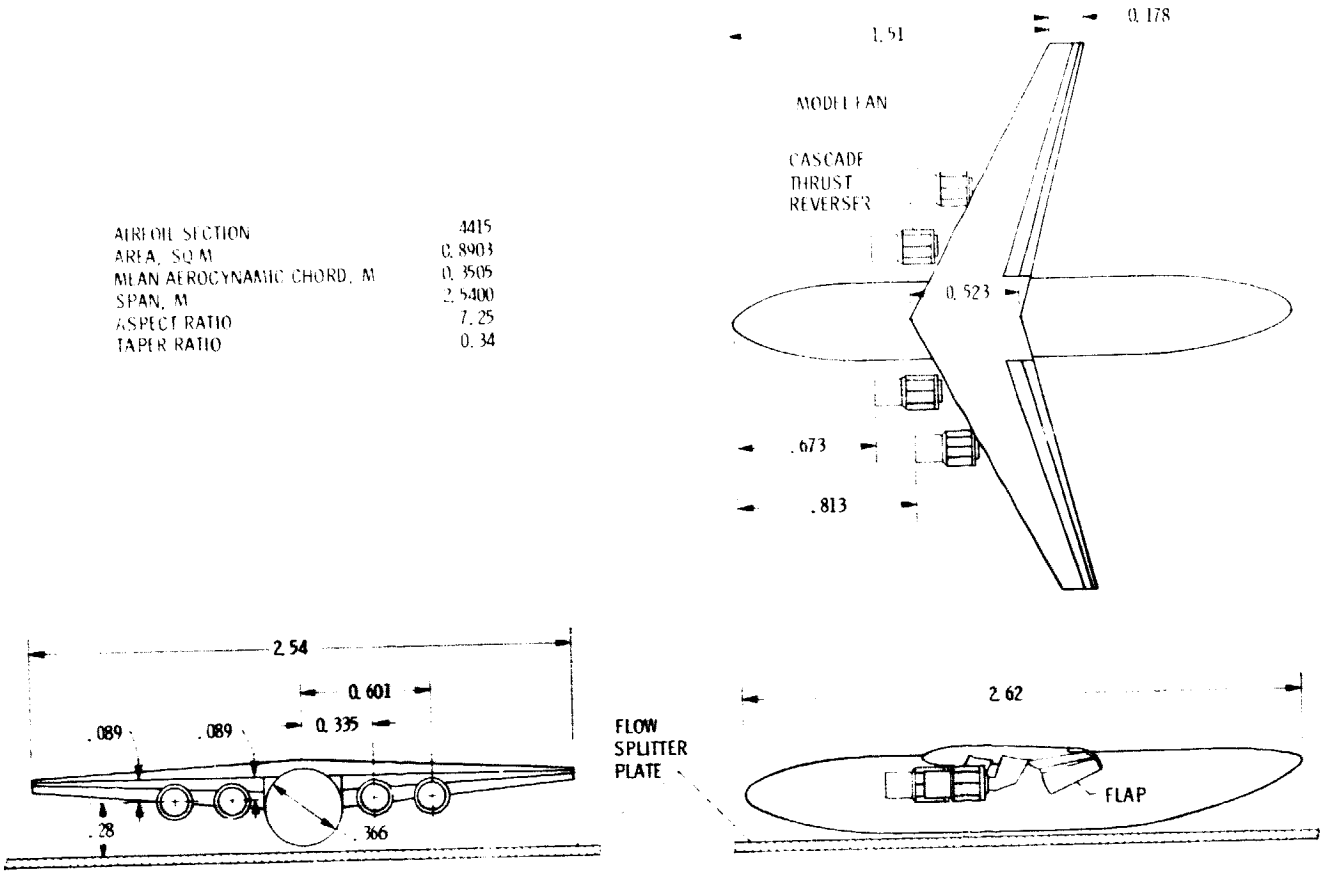

E-8119

Figure 5. - Airplane model including four fan/reverser systems for wind tunnel tests. (All dimensions in meters.)

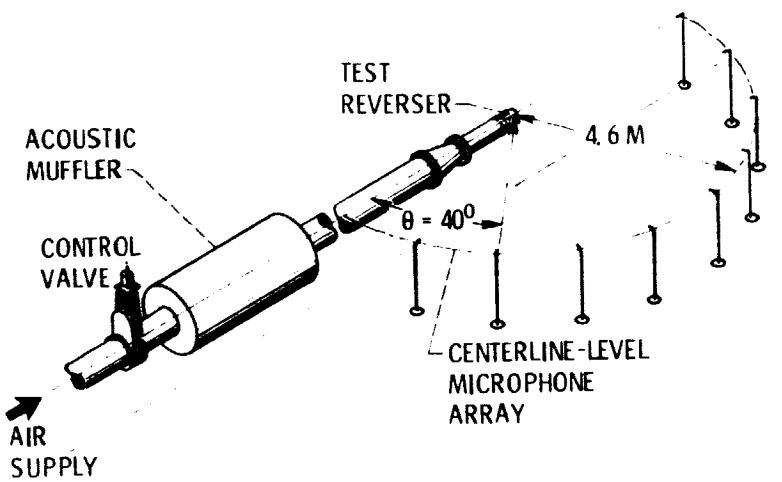

Figure 6. - Schematic diagram of acoustic test stand.

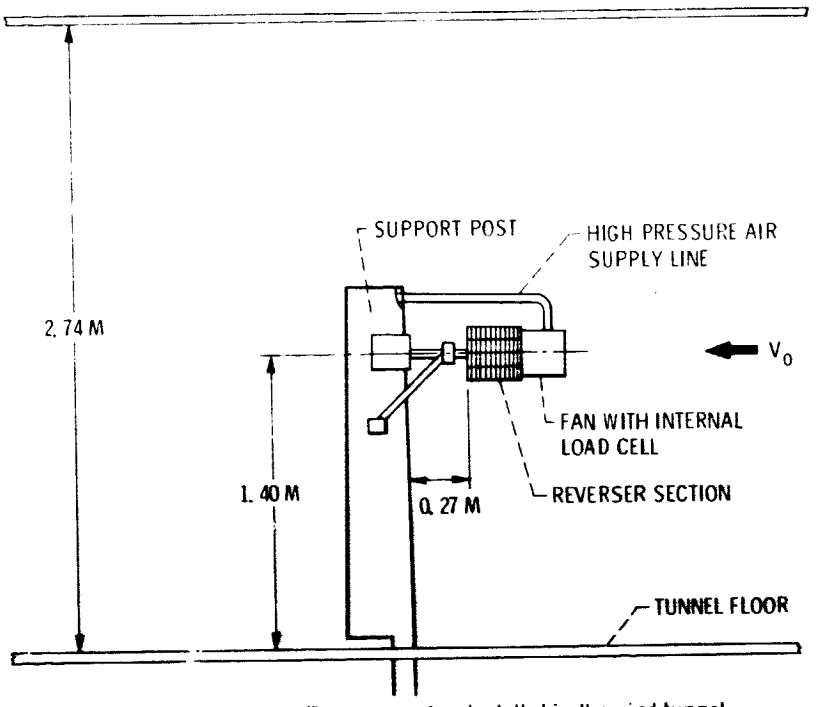

Figure 7. - Isolated fan/Reverser system installed in the wind tunnel.

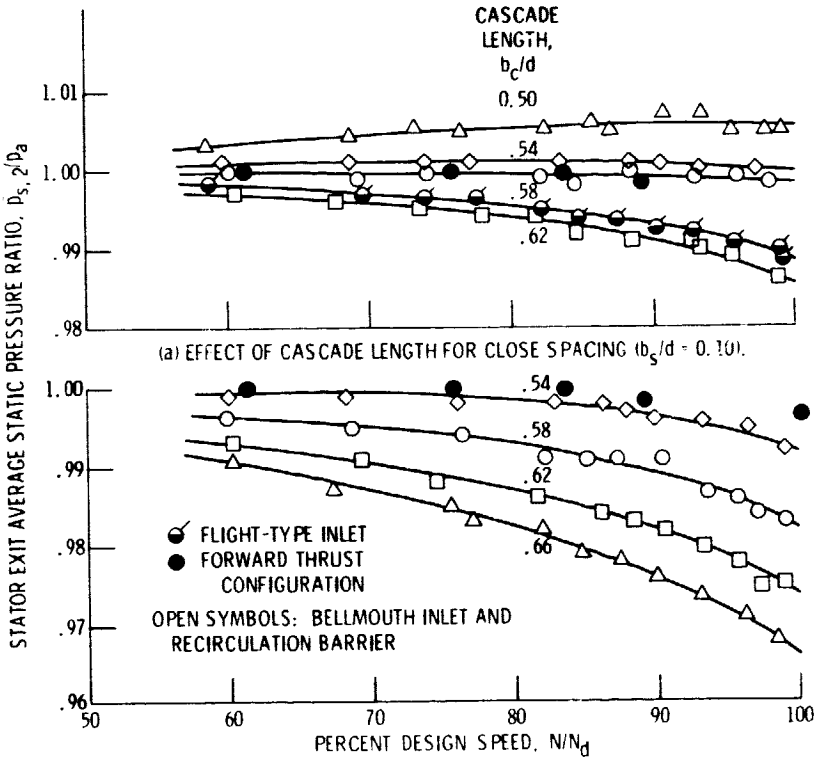

(a) EFFECT OF CASCADE LENGTH FOR CLOSE SPACING (b_s/d = 0.10).

(b) EFFECT OF CASCADE LENGTH FOR LARGE SPACING (b_s/d = 0.52).

Figure 8. - Average stator exit static pressure ratio variation as a function of percent design speed for the fan/reverser model.

E-8119

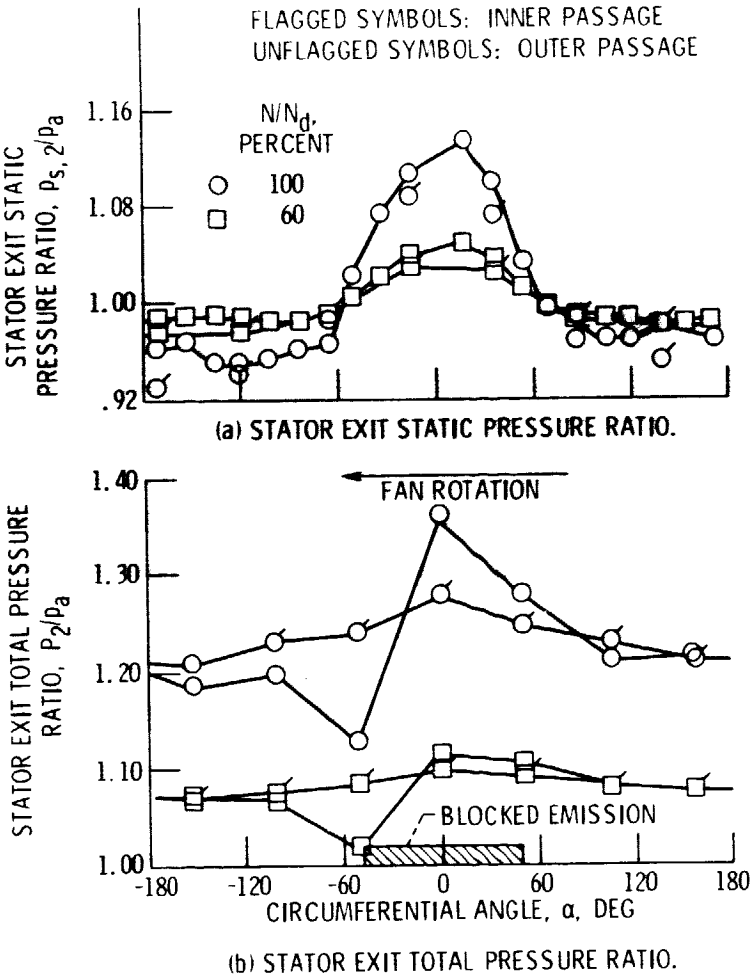

Figure 9. - Stator exit pressure profiles for the fan/reverser model with bellmouth inlet and recirculation barrier. $b_c/d = 0.58$, $b_s/d = 0.10$.

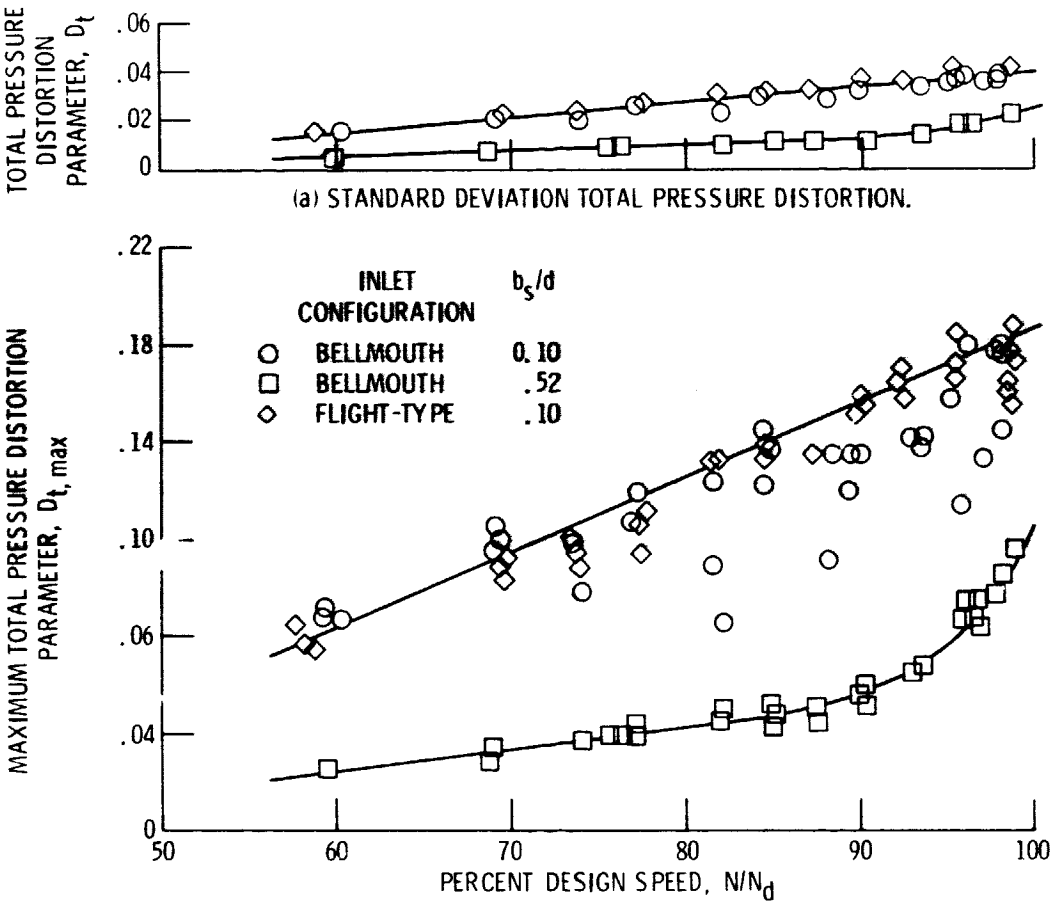

Figure 10. - Variation of pressure distortion parameters as a function of percent design speed for the fan/reverser model. $b_c/d = 0.58$.

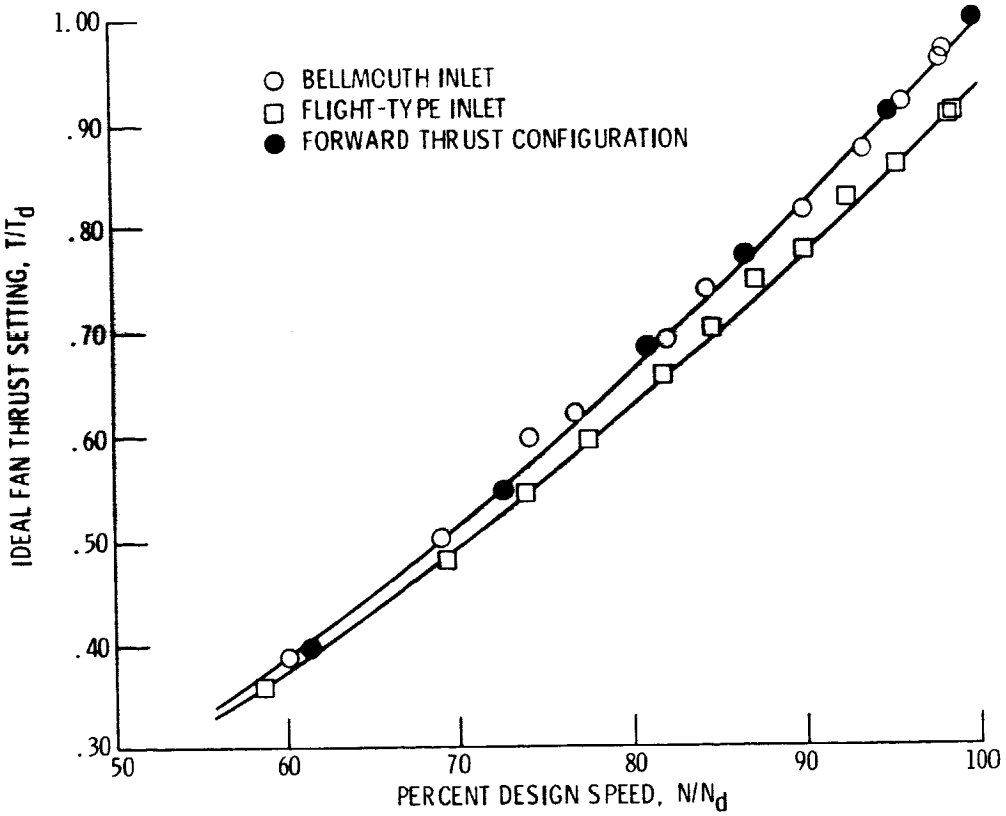

Figure 11. - Variation of ideal fan thrust setting with percent design speed for the fan/reverser model. $b_s/d = 0.10$, $b_c/d = 0.58$.

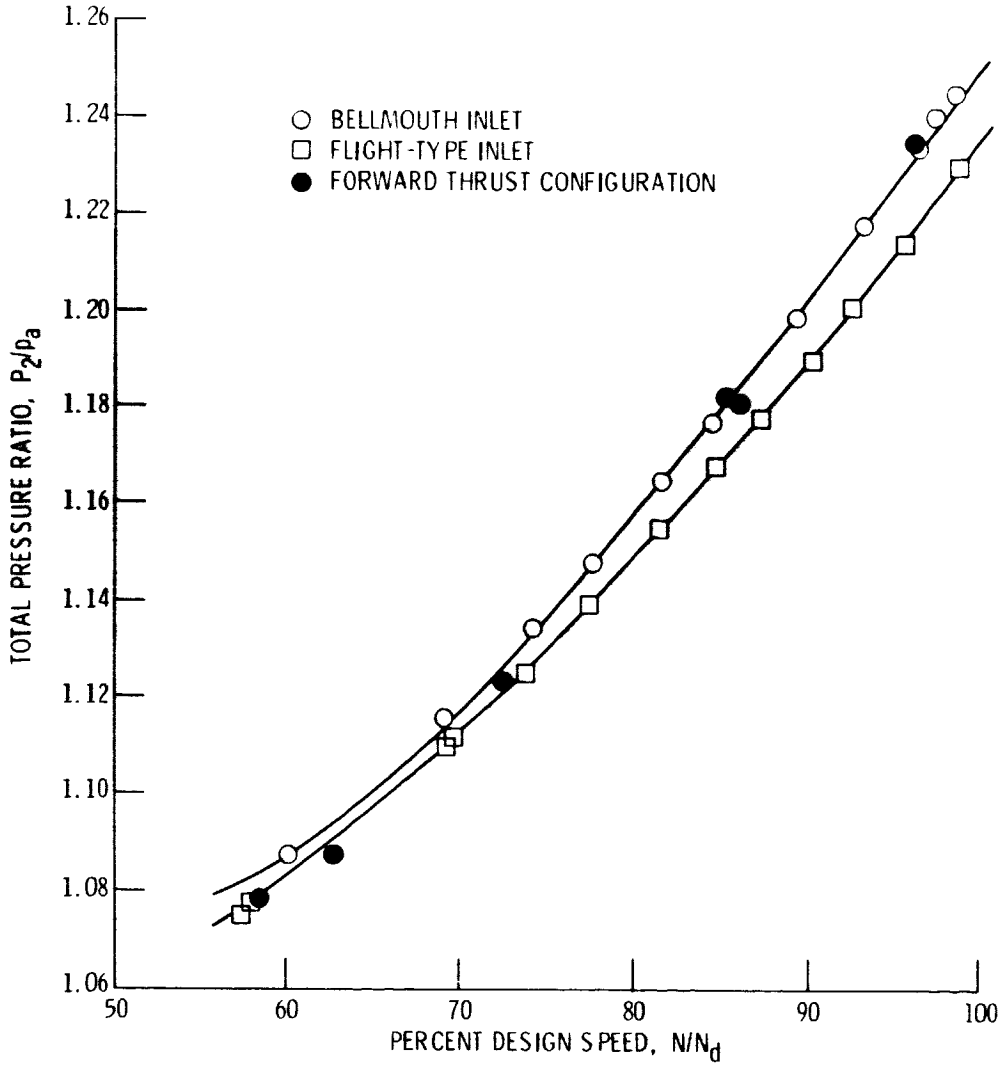

Figure 12. - Variation of fan exit total pressure ratio with percent design speed for the fan/reverser model. $b_s/d = 0.10$, $b_c/d = 0.58$.

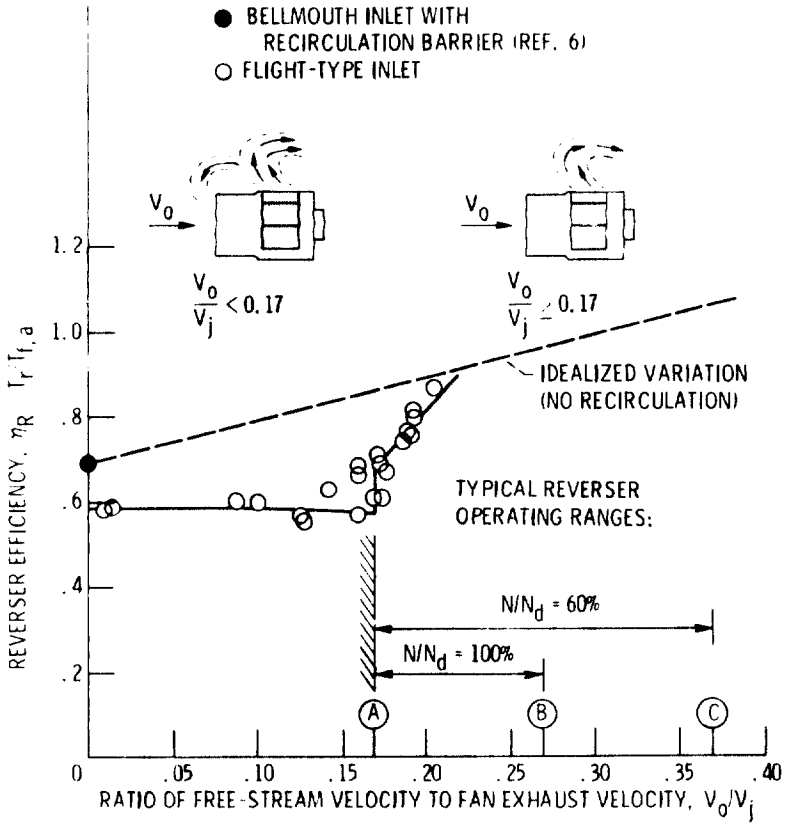

Figure 13. - Isolated thrust reverser efficiency as a function of free-stream-to-exhaust velocity ratio for the fan/reverser model. $b_s/d = 0.10$, $b_c/d = 0.58$.

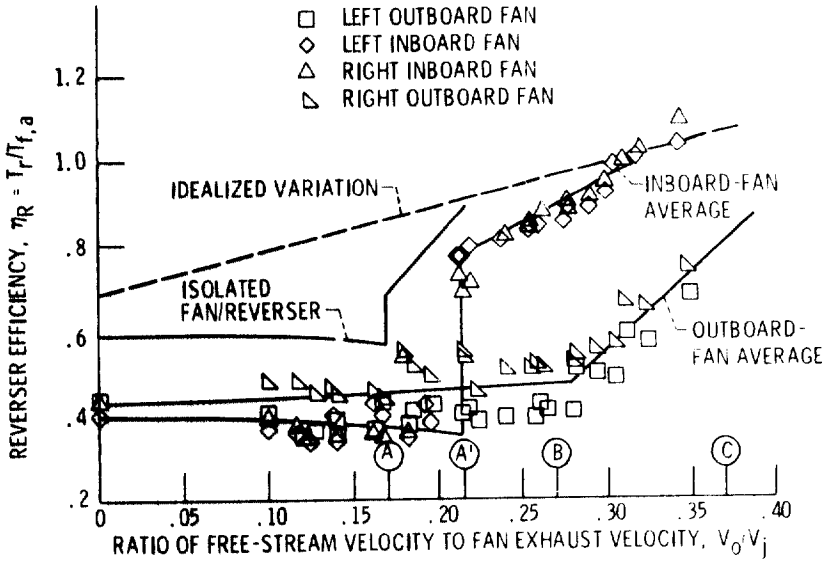

Figure 14. - Installed thrust reverser efficiency as a function of free-stream-to-exhaust velocity ratio for the fan/reverser systems on the airplane model. $b_s/d = 0.10$, $b_c/d = 0.58$.

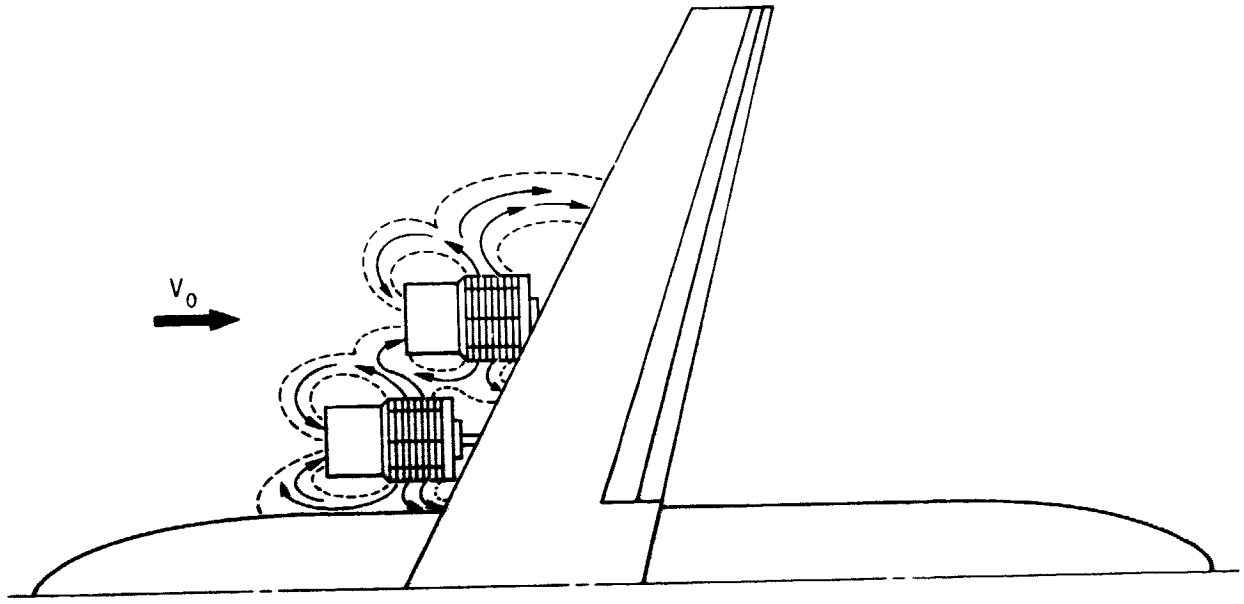

(a) $V_0/V_j < 0.22$.

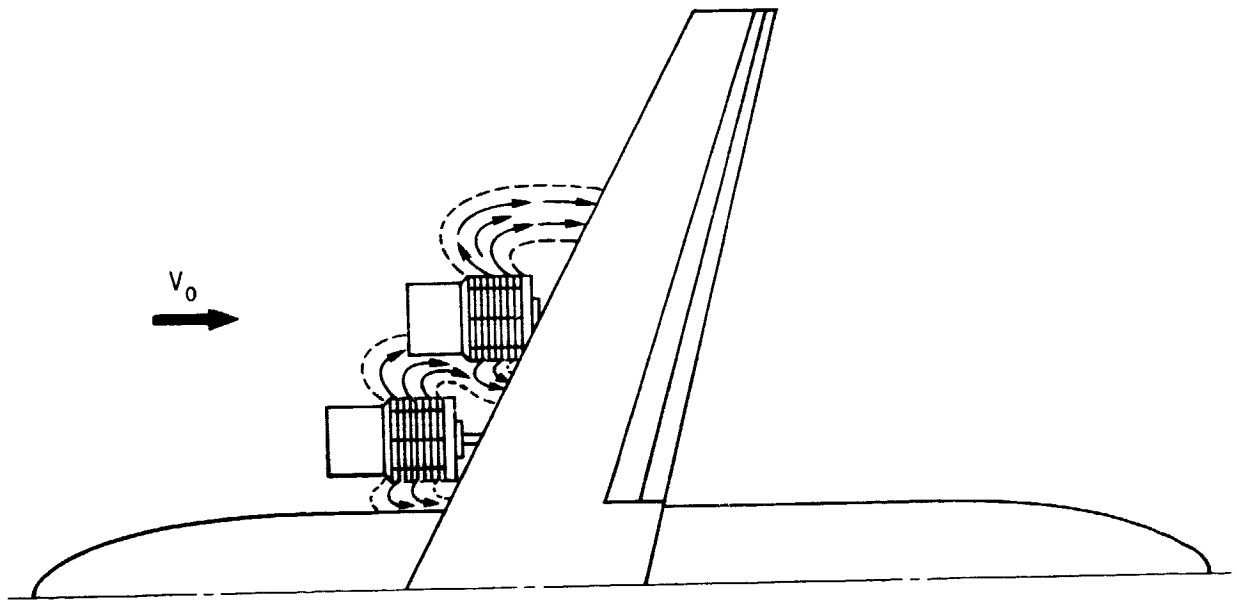

(b) $V_0 \geq 0.22$.

Figure 15. - Reverser exhaust flow patterns for the airplane model for two ranges of values of the free-stream-to-exhaust velocity ratio.

E-8117

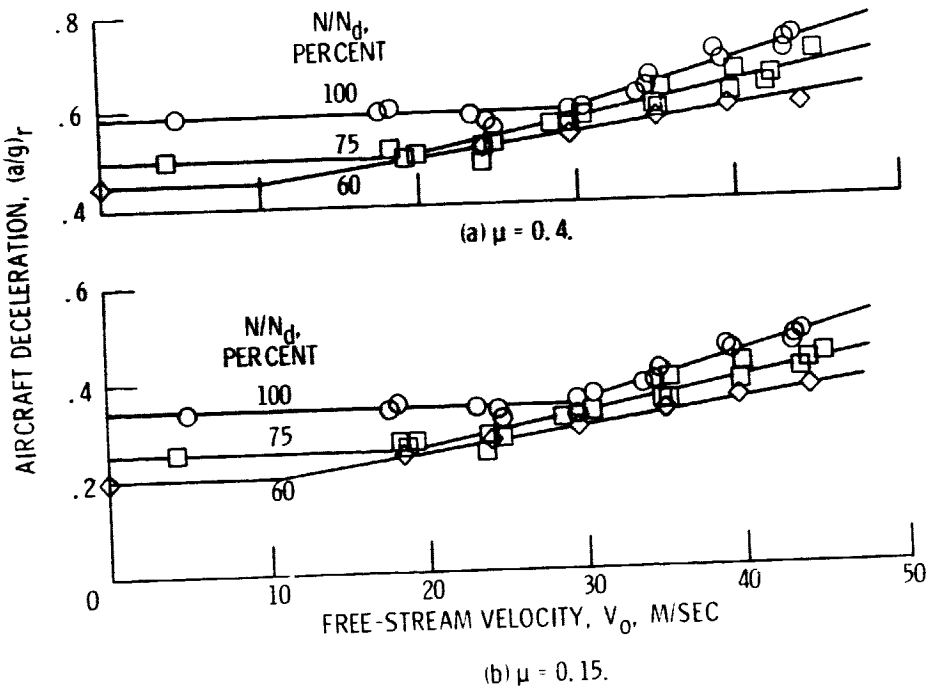

Figure 16. - Variation of calculated full-scale aircraft deceleration as a function of free-stream velocity for two values of runway friction coefficient.

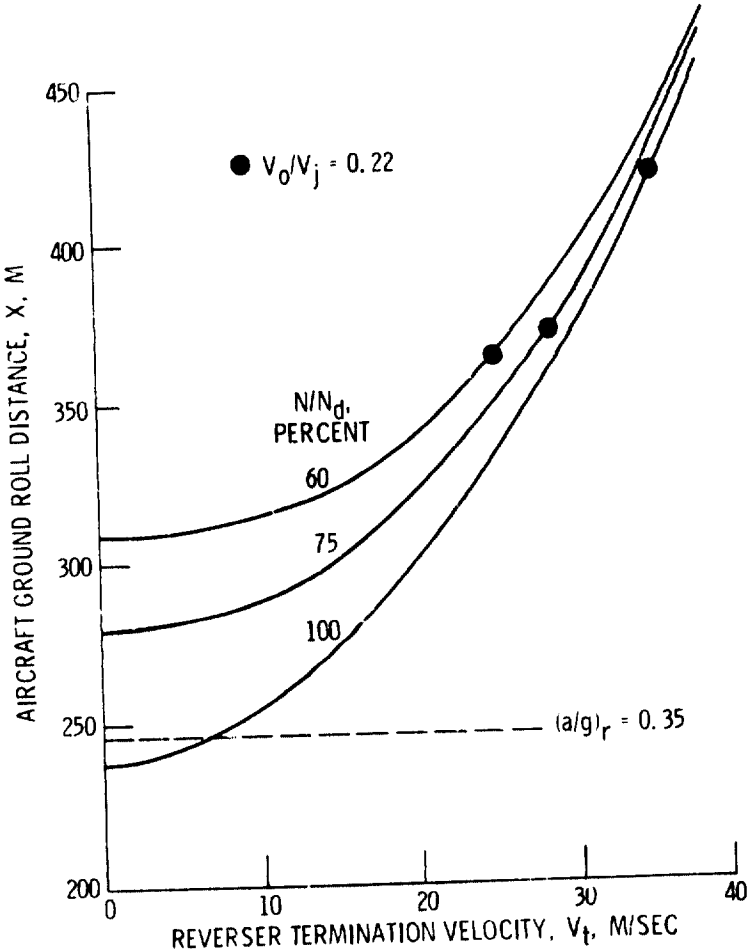

Figure 17. - Variation of calculated ground roll distance with reverser termination velocity. μ = 0.15, V_{td} = 41 m/sec.

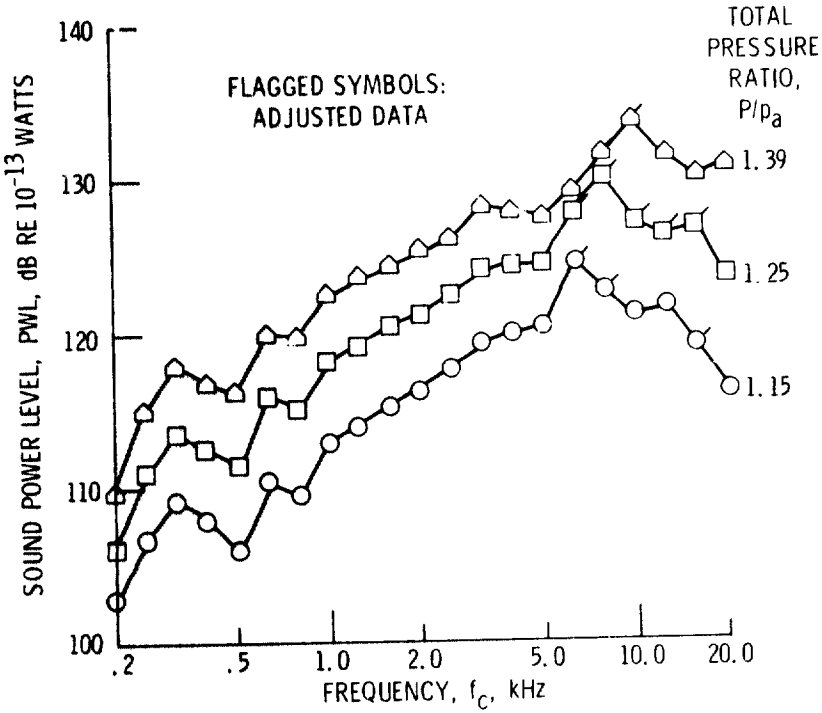

Figure 18. - Thrust reverser adjusted sound power level spectra. b_c/d = 0.58.

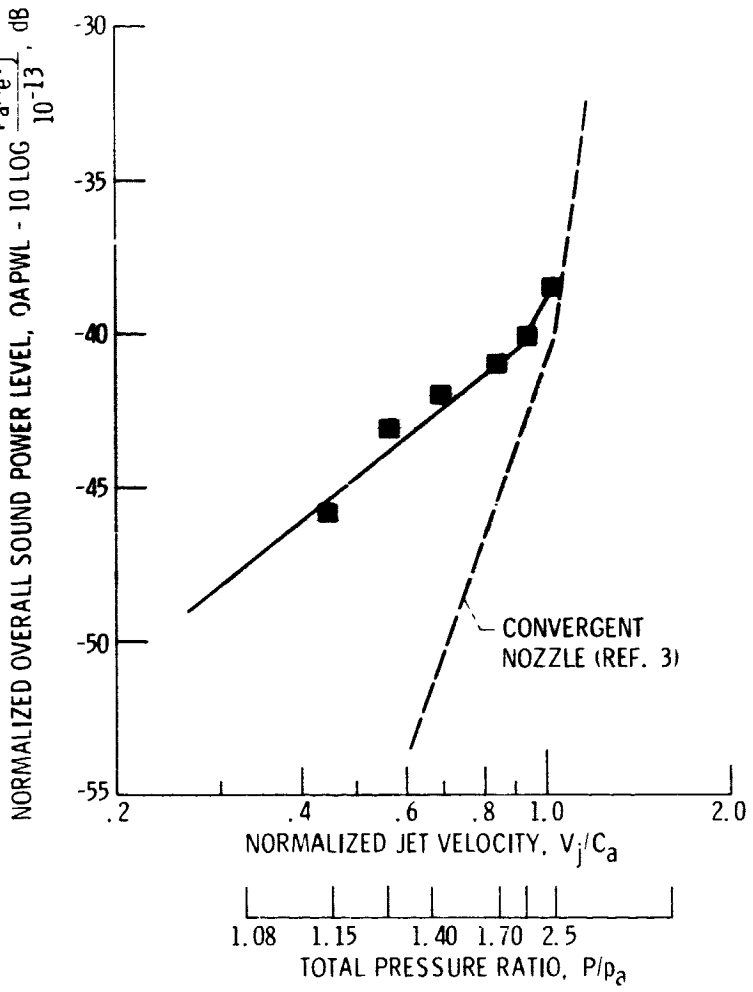

Figure 19. - Normalized overall sound power level for the selected thrust reverser. $b_c/d = 0.58$.

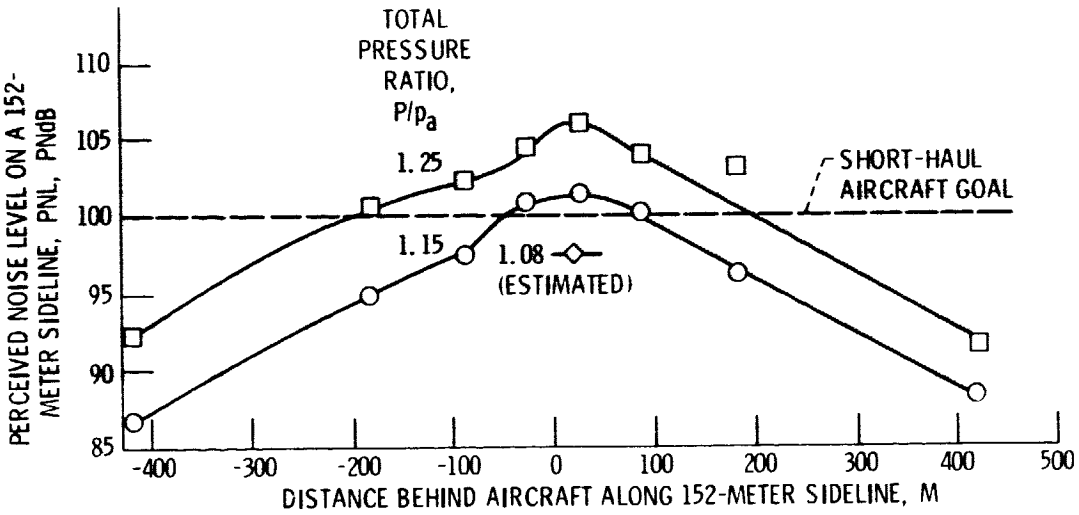

Figure 20. - Sideline perceived noise level from the selected thrust reverser scaled to a 1.96-meter diameter fan. $b_c/d = 0.58$.

E-8117

END

DATE

FILMED

DEC 6 1974